A new near-field phase-correction method for superlens*

Wang Ying-Qi(王瑛琪)[a], Ye Jia-Sheng(叶佳声)[b], Liu Shu-Tian(刘树田)[a], and Zhang Yan(张 岩)[a)b)†]

[a)] *Department of Physics, Harbin Institute of Technology, Harbin* 150001, *China*
[b)] *Department of Physics, Capital Normal University, Beijing* 100048, *China*

(Received 6 April 2012; revised manuscript received 16 April 2013)

A new phase-correction method in a realistic loss superlens imaging system is theoretically predicted. The image resolution is enhanced using the near-field active phase-correction method. Resolvable separation between two slits has been significantly improved to $\lambda/20$ for the symmetrical superlens system and $\lambda/12$ for unsymmetrical system.

Keywords: metamaterials, optical transfer functions, super resolution

PACS: 42.30.Va, 42.30.Lr, 87.57.cf **DOI:** 10.1088/1674-1056/22/11/114202

1. Introduction

For the potential applications in photolithography, many researchers have been dedicated to overcoming the diffraction limit by the superlens in various wavelength regions, from microwave to visible light.[1–6] The diffraction limit comes from the evanescent waves carrying the high spatial frequency information of the object decay in propagating and hardly contributing to the imaging course. For the diffraction limit with the superlens, the permittivity (or permeability) of the superlens needs to be negative, responding to the p-polarization (or s-polarization) illuminating light. However, it is difficult to get negative permeability material at optical frequencies, and the noble metal can present the negative permittivity at optical frequencies. The negative permittivity effect appears during the surface plasmonic oscillations of metals, which couples the high transverse spatial frequency into the imaging course. In this course, the imaginary part of permittivity either corresponds to the loss of energy or influences the image reconstruction on the image plane. To overcome this problem, the beam is spatially shifted using a near-field plate or transmission screen[7,8] to achieve subdiffraction focusing. However, the subwavelength phase plate is quite difficult to fabricate. Recently, the active phase-correction method was introduced by tuning the wavelength of incident light.[9–11] This method can increase the transmission and decrease the error on the image plane. Nonetheless, the incident wavelength cannot be continuously tuned in photolithography. In this paper, we adjust the permittivity instead of the wavelength to achieve the phase correction. Resolvable separation between two slits has been significantly improved to $\lambda/20$ for the symmetrical superlens system and $\lambda/12$ for the unsymmetrical system.

The paper is arranged as follows. In Section 2, we present the theoretical derivation. In Section 3, we utilize this method to achieve a long work distance. At last, we draw a brief conclusion in Section 4.

2. Theory derivation

The field distribution $E_i(x)$ on the image plane of an imaging system can be obtained by the convolution of the spatial frequency spectrum of the field distribution $\tilde{E}_0(k_x)$ on the object plane with the optical transmission function (OTF),

$$E_i(x) = \frac{1}{2\pi}\int_{-\infty}^{+\infty} \tilde{E}_0(k_x)\tau(k_x)\exp(\mathrm{i}xk_x)\,\mathrm{d}k_x, \tag{1}$$

where k_x is the transverse wave vector, $k_z^{(i)}$ is the wave vector in the medium i along the z direction, $k_z^{(i)} = \sqrt{\varepsilon_i k_0^2 - k_x^2}$ with k_0 being the wave number of incident light in a vacuum, and τ denotes the OTF function.

From this equation, it can be found that it needs higher spatial frequency k_x to participate in the imaging process to obtain a more precise image. Therefore, the modulation of OTF must be nearly to 1 for the large regional of k_x and the phase of OTF must remain as small as possible since it corresponds to the loss of the imaging system.

For a near-field superlens imaging system described in Fig. 1, the OTF can be given by the multiplication of transmission coefficient of the metal film and propagation factors through the dielectrics as follows:

$$\tau(k_x) = \frac{t_{1\mathrm{M}}t_{\mathrm{M}1}\exp[\mathrm{i}(k_z^{(1)}d + k_z^{(\mathrm{M})}d)]}{1 - r_{1\mathrm{M}}^2\exp(\mathrm{i}2k_z^{(\mathrm{M})}d)}, \tag{2}$$

where

$$t_{1\mathrm{M}} = \frac{2k_z^{(1)}/\tilde{\varepsilon}_1}{k_z^{(1)}/\tilde{\varepsilon}_1 + k_z^{(\mathrm{M})}/\tilde{\varepsilon}_{\mathrm{M}}},$$

$$t_{\mathrm{M}1} = \frac{2k_z^{(\mathrm{M})}/\tilde{\varepsilon}_{\mathrm{M}}}{k_z^{(1)}/\tilde{\varepsilon}_1 + k_z^{(\mathrm{M})}/\tilde{\varepsilon}_{\mathrm{M}}},$$

*Project supported by the National Basic Research Program of China (Grant No. 2011CB301801) and the National Natural Science Foundation of China (Grant Nos. 10904099 and 11174211).

†Corresponding author. E-mail: yzhang@mail.cnu.edu.cn

© 2013 Chinese Physical Society and IOP Publishing Ltd

are the transmission coefficients from dielectric to metal and from metal to dielectric, and

$$r_{1\mathrm{M}} = \frac{k_z^{(1)}/\widetilde{\varepsilon}_1 - k_z^{(\mathrm{M})}/\widetilde{\varepsilon}_\mathrm{M}}{k_z^{(1)}/\widetilde{\varepsilon}_1 + k_z^{(\mathrm{M})}/\widetilde{\varepsilon}_\mathrm{M}}$$

is the reflection coefficient of dielectric and metal, ε_i is the permittivity of medium i, d is the thickness of the metal film, and the dielectric thickness is $d/2$. Equation (2) can be expanded as:

$$\tau(k_x) = \frac{t_{1\mathrm{M}}t_{\mathrm{M}1}\exp[\mathrm{i}(k_z^{(1)}d + k_z^{(\mathrm{M})}d)]}{1 - r_{1\mathrm{M}}^2\exp(\mathrm{i}2k_z^{(\mathrm{M})}d)} = \frac{4(k_z^{(\mathrm{M})}k_z^{(1)}/\widetilde{\varepsilon}_1\widetilde{\varepsilon}_\mathrm{M})\exp[\mathrm{i}(k_z^{(1)}d + k_z^{(\mathrm{M})}d)]}{(k_z^{(1)}/\widetilde{\varepsilon}_1 + k_z^{(\mathrm{M})}/\widetilde{\varepsilon}_\mathrm{M})^2 - (k_z^{(1)}/\widetilde{\varepsilon}_1 - k_z^{(\mathrm{M})}/\widetilde{\varepsilon}_\mathrm{M})^2\exp(\mathrm{i}2k_z^{(\mathrm{M})}d)}. \quad (3)$$

From Eq. (3), it can be concluded that if both the index parts of numerator and denominator approach 1, the OTF will be a constant equal to 1 no matter how the permittivity and transverse spatial frequency change. Thus, the task of the superlens system design is to find the suitable permittivity of dielectric and metal for making the index part of the OTF approach 1.

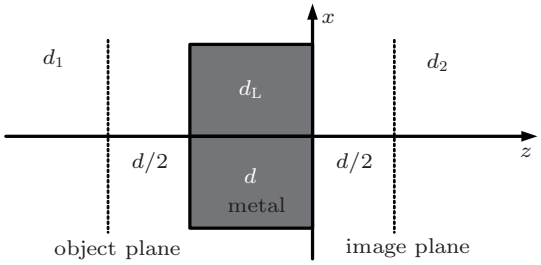


Fig. 1. Schematic geometry of a superlens system. d_i $(i = 1, 2, L)$ represents the medium i, d_1 and d_2 stand for dielectrics, and d_L for a metallic lens. d denotes the metal thickness, and $2d$ is the work distance of this superlens system. The object is two slits.

For the high transverse spatial frequency larger than k_0, all the index parts are attenuation parts. In order to keep the attenuation as small as possible, the thickness of the metal and dielectrics should be less than $1/10$ of the wavelength of the incident light in the medium. In this paper, the wavelength of incident light is selected as 365 nm in vacuum. The dielectric is polymethyl methacrylate (PMMA) whose permittivity is $2.3014 + 0.0014\mathrm{i}$. Therefore, the thickness d should satisfy $d < \lambda/(10\sqrt{\varepsilon_1})$, and is chosen as 10 nm in this work.

At the high transverse spatial frequency limit, the wave vectors in the z direction inside medium i are approximated as its first order

$$k_z^{(i)} = \sqrt{\widetilde{\varepsilon}_i\mu k_0^2 - k_x^2} = \mathrm{i}k_x\sqrt{1 - \frac{\widetilde{\varepsilon}_i\mu k_0^2}{k_x^2}} = \mathrm{i}\left(k_x - \frac{\widetilde{\varepsilon}_i\mu k_0^2}{2k_x}\right).$$

For the thin metal film and dielectric, the approximation is substituted into the index part of the OTF. Two error functions are introduced to describe the error of the index parts,

$$\Delta_1 = \exp[\mathrm{i}(k_z^{(1)}d + k_z^{(\mathrm{M})}d)] - 1, \quad (4)$$

$$\Delta_2 = \exp(\mathrm{i}2k_z^{(\mathrm{M})}d) - 1. \quad (5)$$

Thus, the OTF can be expressed with the error functions as

$$\tau(k_x) = \frac{4(k_z^{(\mathrm{M})}k_z^{(1)}/\widetilde{\varepsilon}_1\widetilde{\varepsilon}_\mathrm{M})(1+\Delta_1)}{(k_z^{(1)}/\widetilde{\varepsilon}_1 + k_z^{(\mathrm{M})}/\widetilde{\varepsilon}_\mathrm{M})^2 - (k_z^{(1)}/\widetilde{\varepsilon}_1 - k_z^{(\mathrm{M})}/\widetilde{\varepsilon}_\mathrm{M})^2(1+\Delta_2)} = \frac{4(k_z^{(\mathrm{M})}k_z^{(1)}/\widetilde{\varepsilon}_1\widetilde{\varepsilon}_\mathrm{M})(1+\Delta_1)}{2(k_z^{(\mathrm{M})}k_z^{(1)}/\widetilde{\varepsilon}_1\widetilde{\varepsilon}_\mathrm{M})(2+\Delta_2) - [(k_z^{(1)}/\widetilde{\varepsilon}_1)^2 + (k_z^{(\mathrm{M})}/\widetilde{\varepsilon}_\mathrm{M})^2]\Delta_2}. \quad (6)$$

The OTF should remain 1 for high spatial frequency limit, so the error functions of the index part should satisfy the following limit:

$$\lim_{\tau\to 1}\frac{\Delta_1}{\Delta_2} = -\frac{[(k_z^{(1)}/\widetilde{\varepsilon}_1) - (k_z^{(\mathrm{M})}/\widetilde{\varepsilon}_\mathrm{M})]^2}{4(k_z^{(\mathrm{M})}k_z^{(1)}/\widetilde{\varepsilon}_1\widetilde{\varepsilon}_\mathrm{M})}. \quad (7)$$

From the definition of the error function, the ratio of two error functions can be expressed by

$$\frac{\Delta_1}{\Delta_2} = \frac{\exp[\mathrm{i}(k_z^{(1)}d + k_z^{(\mathrm{M})}d)] - 1}{\exp(\mathrm{i}2k_z^{(\mathrm{M})}d) - 1}. \quad (8)$$

From Eqs. (7) and (8), the permittivities of this system can be decided. In this work, only the permittivity of metal is adjusted for achieving high resolution. In the real design, the permittivity of dielectric or both of them can be adjusted.

Figure 2 gives the ideal metal permittivity curve calculated by Eqs. (7) and (8). The wavelength of the incident light is 365 nm in a vacuum. The thickness of the metal film d is chosen to be 10 nm and the thickness of the separate dielectric is $d/2$. The separate dielectric is the PMMA, whose permittivity is $2.3014 + 0.0014\mathrm{i}$ at the incident wavelength. The blue line describes the real part of the metal permittivity, and the green line is the imaginary part. The horizontal ordinate is the transverse spatial frequency. It can be found that the real part of the permittivity has a resonance at $k_x = 1.517k_0$ and approaches 2.40, while the imaginary part approaches zero. The resonance at $k_x = 1.517k_0$ is produced by the change of the

propagating mode to the evanescent mode. From this figure, it can be found that the metal film is an anisotropic material. For different transverse spatial frequencies, the metal permittivity is required to be different. This kind of anisotropic material is difficult to prepare, so a certain permittivity should be chosen to make the OTF close to 1.

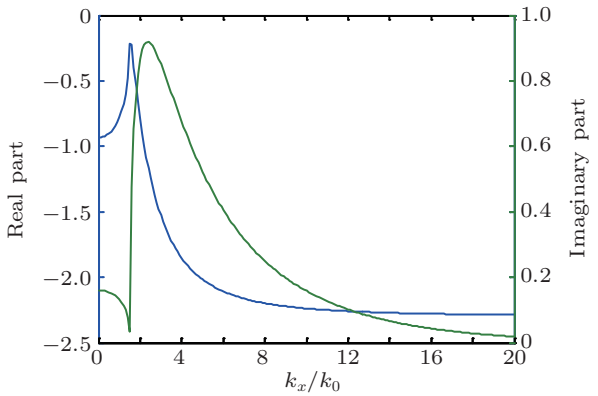


Fig. 2. (color online) The ideal metal permittivity versus the transverse spatial frequency. The blue line presents the real part of the permittivity and the green line describes the imaginary part of the permittivity.

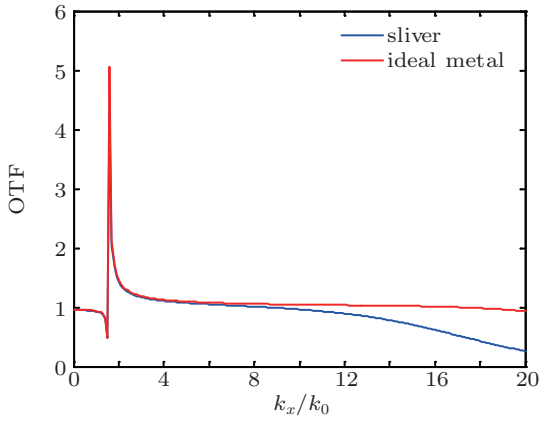


Fig. 3. (color online) OTF curves for the sliver (blue line) and ideal metal (red line).

Figure 3 plots the OTF curves calculated by Eq. (2) using the real metal sliver (blue line) whose permittivity is $-2.4012+0.2488\mathrm{i}$. All other parameters are the same as those in Fig. 2. The OTF of a sliver superlens is close to 1 when $k_x < 10k_0$ except the resonance at $k_x = 1.517k_0$, but it drops to 0.2622 quickly after $k_x > 10k_0$. As a result, the middle permittivity at the transverse spatial frequency $k_x = 15k_0$ is chosen as $\varepsilon_\mathrm{m} = -2.275+0.0537\mathrm{i}$. The red line shows the OTF of ideal metal whose permittivity is $-2.275+0.0537\mathrm{i}$. From this figure, it can be found that the OTF for ideal metal is closer to 1 than the real metal at high transverse spatial frequency. In Fig. 3, the part of OTF is bigger than 1 because that the OTF is a function of the amplitude. The amplitude transmission function would be over 1 near the transmission resonant peak. The parameters are chosen using Eqs. (7) and (8), which are approximated as the first order of Eq. (2). The curve in Fig. 3 is calculated by Eq. (2), which is not approximated. The parameters in Fig. 2 and the OTF in Fig. 3 have different sources, which is the main reason for the OTF over 1.

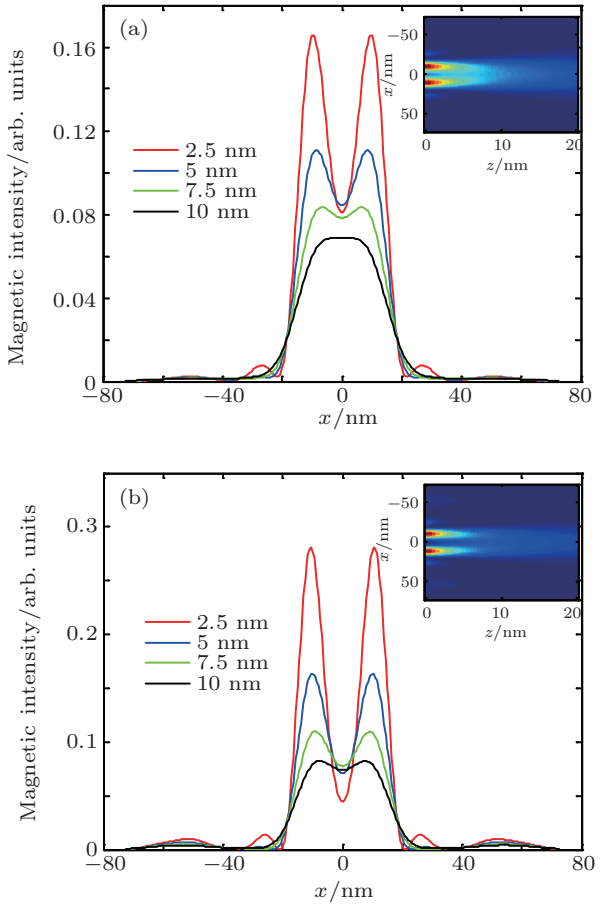


Fig. 4. (color online) Magnetic intensity distributions of two slits through (a) the sliver and (b) ideal metal superlens system. The permittivity of sliver is $-2.4012+0.2488\mathrm{i}$ at the incident light wavelength of 365 nm, and the permittivity of ideal metal is $-2.275+0.0537\mathrm{i}$. The thickness of metal film d is 10 nm; the thickness of separate dielectric is $d/2$; the distance between two slits is 18 nm; the width of slit is 15 nm. The red line represents the magnetic intensity distribution at 2.5 nm away from the metal, blue line at 5 nm, green line at 7.5 nm, and black line at 10 nm. The insets show the field distributions near the metal.

Figure 4(a) shows the magnetic intensity distributions of two slits through a sliver imaging system at different distances away from the metal, calculated with the FDTD method. The distance between two slits is 18 nm and the width of slit is 15 nm. The red line represents the magnetic intensity distribution at 2.5 nm away from the metal, blue line at 5 nm, green line at 7.5 nm, and black line at 10 nm. The blue line corresponds to the image on the theoretical image plane. The p–p distance at the theoretical image plane is 19 nm. The inset presents the field distribution near the metal. Figure 4(b) shows the magnetic intensity through an ideal metal imaging system, whose permittivity is calculated to be $\varepsilon_\mathrm{m} = -2.275+0.0537\mathrm{i}$ by virtue of Eqs. (7) and (8) at $k_x = 15k_0$. All other parameters are the same as those in Fig. 4(a). The p–p distance at the theoretical image plane is 21 nm. Both p–p distances on theoretical image plane are longer than the dis-

tance of two slits. The superlens system has no change in the x direction, but has the metal lens whose permittivity is minus in the z direction. The whole superlens system is regarded as an anisotropic medium. This phenomenon is caused by diffraction in an anisotropic medium.

The conventional visibility $V = (I_{\max} - I_{\min})/(I_{\max} + I_{\min})$ of a transmission field is used to evaluate the imaging ability of the superlens. On the theoretical image plane, the visibility of sliver superlens is 0.1338, but the visibility of ideal metal is 0.3966. The depth of field is defined by the distance from the metal to a plane with visibility of 0.2. Therefore, the sliver superlens' depth of field is only 4 nm, but the ideal metal's depth of field can achieve 7.5 nm. The resolution is defined by the distance of two slits when the visibility is larger than 0.4 on the theoretical image plane. The resolution of ideal metal achieves $\lambda/20$, but the resolution of sliver is only $\lambda/15$. Compared with Fig. 4(a), the imaging quality of the ideal metal in Fig. 4(b) is much better than the real metal. The image obtained by the ideal metal has higher contrast and longer focal depth. It is proved that this optimization of the permittivity of metal can help us design a better superlens.

3. Imaging distance

Although the symmetric structure near field superlens can get a better image, the different imaging distance generated by the unsymmetrical imaging system can transcribe the image into the photoresist better. For an unsymmetrical imaging system, the OTF becomes

$$\tau(k_x) = \frac{t_{1\mathrm{M}} t_{\mathrm{M}1} \exp[\mathrm{i}(k_z^{(1)} d_1 + k_z^{(\mathrm{M})} d + k_z^{(1)} d_2)]}{1 - r_{1\mathrm{M}}^2 \exp(\mathrm{i}2k_z^{(\mathrm{M})} d)} = \frac{4(k_z^{(\mathrm{M})} k_z^{(1)}/\widetilde{\varepsilon}_1 \widetilde{\varepsilon}_{\mathrm{M}}) \exp[\mathrm{i}(k_z^{(1)} d_1 + k_z^{(\mathrm{M})} d + k_z^{(1)} d_2)]}{(k_z^{(1)}/\widetilde{\varepsilon}_1 + k_z^{(\mathrm{M})}/\widetilde{\varepsilon}_{\mathrm{M}})^2 - (k_z^{(1)}/\widetilde{\varepsilon}_1 - k_z^{(\mathrm{M})}/\widetilde{\varepsilon}_{\mathrm{M}})^2 \exp(\mathrm{i}2k_z^{(\mathrm{M})} d)}, \tag{9}$$

where d_1 is the distance from the object to the metal, and d_2 is the imaging distance from the metal.

In this case, the metal permittivity is required to satisfy

$$\frac{\Delta_1}{\Delta_2} = \frac{\exp[\mathrm{i}(k_z^{(1)} d_1 + k_z^{(1)} d_2 + k_z^{(\mathrm{M})} d)] - 1}{\exp(2\mathrm{i}k_z^{(\mathrm{M})} d) - 1}. \tag{10}$$

Figure 5 presents the metal permittivity curve calculated by Eqs. (7) and (10) for the unsymmetrical structure. The thickness of separate dielectric d_1 is 5 nm, and the imaging distance d_2 is 15 nm. All other parameters are equal to those in Fig. 2. The middle permittivity at the transverse spatial frequency k_x=12k_0 is chosen, i.e., $\varepsilon_{\mathrm{m}} = -1.793 + 0.001801\mathrm{i}$.

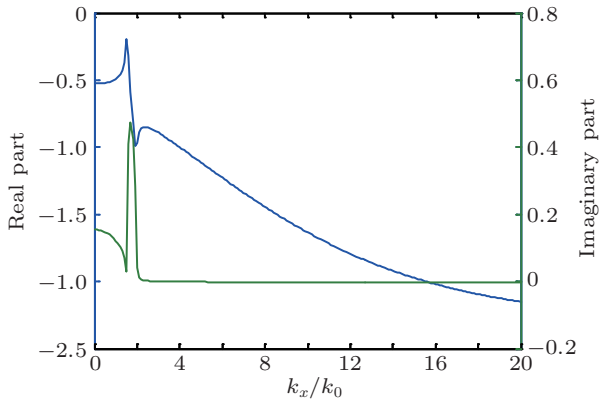


Fig. 5. (color online) Ideal metal permittivity versus the transverse spatial frequency for unsymmetrical structure. The blue line represents the real part of permittivity, and the green line represents the imaginary part of permittivity.

Figure 6 shows the curves calculated by Eq. (2) using the sliver (blue line) and ideal metal (red line). The real metal is sliver with permittivity $\varepsilon_{\mathrm{m}} = -2.4012 + 0.2488\mathrm{i}$. The ideal metal's permittivity is $-1.793 + 0.001801\mathrm{i}$. All other parameters are the same as those in Fig. 2. From this figure, it can be found that the OTF for ideal metal system is larger than the real metal system at high transverse spatial frequency, from $2k_0$ to $10k_0$. The resonance of ideal metal at $k_x = 1.517k_0$ is higher than that of sliver because the ideal metal has a small imaginary part. However, there is one more resonance appearing at $k_x = 12k_0$, which comes from the permittivity being chosen at this transverse spatial frequency. This peak is the body resonant peak of metal. Unlike the first surface resonant peak of metal, this peak attenuates faster than the first peak when the imaginary part of metal permittivity increases. In Fig. 6, because the imaginary part of metal permittivity is smaller than sliver, this peak appears. This resonance peak indicates the cut-off frequency of transverse spatial frequency. The interaction of two resonance peaks increases the transmission whose frequency is between the two peaks.

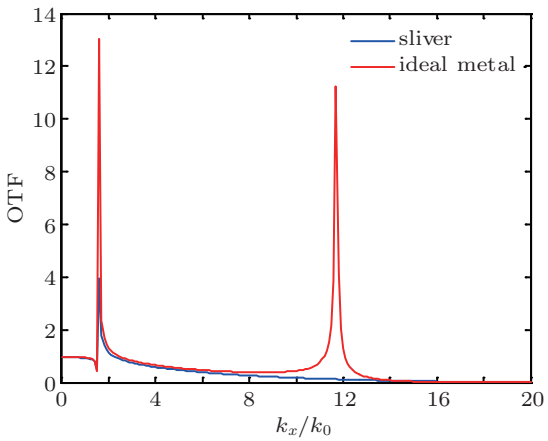


Fig. 6. (color online) OTF curves for the real metal (blue line) and ideal metal (red line) for unsymmetrical system.

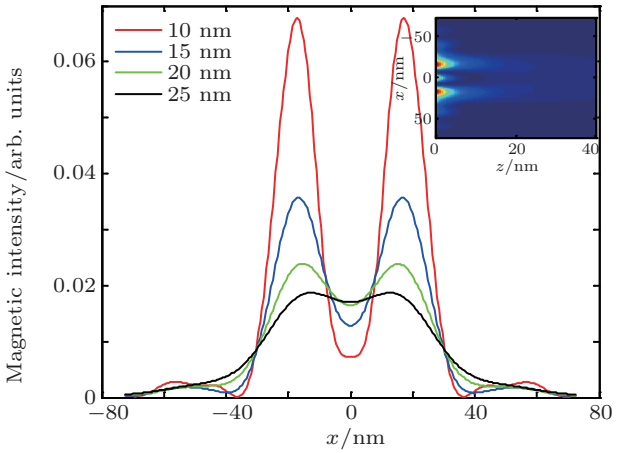


Fig. 7. (color online) Magnetic intensity distributions of two slits through an ideal metal imaging system with unsymmetrical structure. The permittivity of ideal metal is $-1.793+0.001801\mathrm{i}$ at the incident light wavelength of 365 nm. The thickness of metal film d is 10 nm; the thickness of separate dielectric is $d/2$; the distance of two slits is 30 nm; the width of one slit is 15 nm. The inset presents the field distribution near the metal.

Figure 7 shows the magnetic intensity distributions of two slits through an ideal metal imaging system with unsymmetrical structure, calculated with the FDTD method. The metal permittivity is chosen as $\varepsilon_{\mathrm{m}} = -1.793+0.001801\mathrm{i}$ at the incident light wavelength of 365 nm. The distance of two slits is 30 nm, and the width of one slit is 15 nm. The red line describes the magnetic distribution at 10 nm away from the metal, blue line at 15 nm, green line at 20 nm, and black line at 25 nm. The blue line corresponds to the magnetic distribution on the theoretical image plane. The p–p distance at the theoretical image plane is 34 nm. This phenomenon has the same reason as that in Fig. 4. The propagating distance of light in the unsymmetrical system is longer than in the symmetrical system, which causes a more obvious broadening effect than in Fig. 4. The two slits can be effectively distinguished and the visibility is 0.4725. The depth of field can achieve 20 nm. As the OTF in Fig. 6 is not as good as that in Fig. 3, the resolution of ideal metal imaging system is reduced to $\lambda/12$.

4. Conclusions

In conclusion, we theoretically predict a new phase-correction method in a realistic lossy superlens imaging system. In a metal superlens system, resolvable separation between two slits is significantly improved to $\lambda/20$ for the symmetrical superlens system and $\lambda/12$ for the unsymmetrical system. This near-field phase-correction method can be extended to the development of a high-performance superlens for photolithography.

References

[1] Pendry J B 2000 *Phys. Rev. Lett.* **85** 3966
[2] Smith D R, Padilla W J, Vier D C, Nemat-Nasser S C and Schultz S 1999 *Phys. Rev. Lett.* **84** 4184
[3] Yen T J, Padilla W J, Fang N, Vier D C, Smith D R, Pendry J B, Basov D N and Zhang X 2000 *Science* **303** 1494
[4] Taubner T, Korobkin D, Urzhumov Y, Shvets G and Hillenbrand R 2006 *Science* **313** 1595
[5] Fang N, Lee H, Sun C and Zhang X 2005 *Science* **308** 534
[6] Yang X, Liu Y, Ma J, Cui J, Xing H, Wang W, Wang C and Luo X 2008 *Opt. Express* **16** 19686
[7] Grbic A, Jiang L and Merlin R 2008 *Science* **320** 511
[8] Markley L, Wong A M H, Wang Y and Eleftheriades G V 2008 *Phys. Rev. Lett.* **101** 113901
[9] Lee K, Park H, Kim J, Kang G and Kim K 2008 *Opt. Express* **16** 1711
[10] Lee K, Jung Y, Kang G, Park H and Kim K 2009 *Appl. Phys. Lett.* **94** 101113
[11] Lee K, Jung Y and Kim K 2009 *Phys. Rev. B* **80** 033109